CORNELL UNIVERSITY

Center for Radiophysics and Space Research

ITHACA, N. Y.

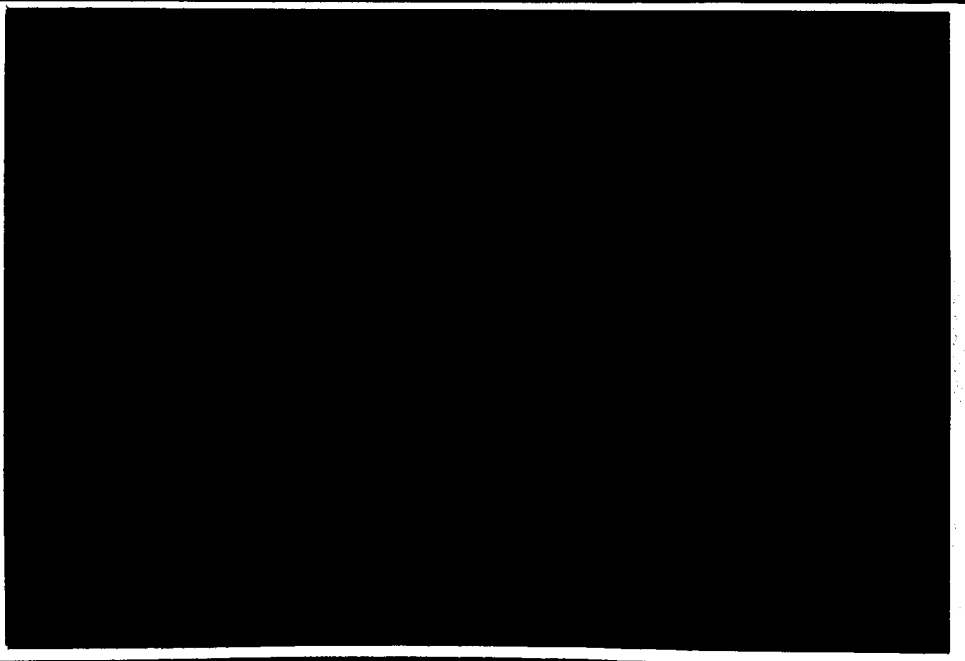

CORNELL UNIVERSITY

CENTER FOR RADIOPHYSICS AND SPACE RESEARCH

Ithaca, N.Y. 14850

July, 1971

CRSR # 456

EFFECTS OF SURFACE ROUGHNESS ON THE PHOTOMETRIC PROPERTIES OF MARS

J. Veverka

L. Wasserman

Laboratory for Planetary Studies

Center for Radiophysics and Space Research

Cornell University, Ithaca, New York

Abstract

Starting with a macroscopically flat surface which at each point scatters according to the Minnaert law with exponent k, we investigate the photometric effects of increasing the large-scale roughness of the surface. It is found that the photometric properties of macroscopically rough surfaces can still be described by the Minnaert law, but with an exponent k*, in general not equal to k. In fact, examples are given where k* differs considerably from k. Therefore observed values of the Minnaert exponent cannot be used to infer the small-scale surface properties of Mars (or of any planet) unless proper allowance is made for the photometric effects of large-scale roughness. The azimuthal dependence of k* provides a sensitive test for the importance of these effects.

1. Introduction:

Young and Collins (1971) have shown that the scattering properties of the surface of Mars can be conveniently dealt with in terms of the Minnaert law

$$B \cos \varepsilon = B_o \, (\cos i \cos \varepsilon)^k$$

where $B(i,\varepsilon,\alpha)$ is the apparent surface brightness at an angle of incidence i, an angle of observation ε, and a phase angle α; $B_o(\alpha)$ and $k(\alpha)$ are the two Minnaert parameters which describe the scattering properties of the surface. Using Mariner 6 and 7 far encounter photographs, Young and Collins have evaluated these parameters for five Martian regions at a phase angle of 22°. They find k's ranging from 0.46-0.48 for the "center of Syrtis Major" to 0.63-0.71 for the bright region Ophir.

At small phase angles values of k between 0.5 and 0.7 are typical for dark, particulate surfaces with negligible large-scale roughness: the lower values being associated with loose, porous powders, while the higher values are characteristic of more compact surfaces. (Frosts, and other high albedo surfaces in which multiple scattering is dominant, tend to have large values of k ($\gtrsim$ 1) even at small phase angles). Thus the observed variations in k suggest the possibility of photometrically mapping the texture of the surface of Mars, and even studying the effects of seasonal changes in particular areas. However, before apparent k values can be used to infer

small scale surface properties, allowance must be made for the effects of large scale roughness, since it is possible to change the apparent k by changing the large scale roughness of the surface without changing either its texture or composition. It is the purpose of this paper to study these effects in detail.

2. The Surface Roughness Model

The general problem of scattering from a randomly rough surface is prohibitively difficult. Basically, one wishes to know for each scattering geometry what portions of the surface are both illuminated and seen. At all such points one must first determine the local scattering angles, and then the amount of scattered light (specified by a given scattering law) in the direction of the observer. The problem is further complicated if the surface material is bright enough for shadows due to large scale roughness to be altered significantly by multiple reflections.

Lacking a solution to the general problem we shall use a contrived, but convenient model of surface roughness first introduced by Hämeen-Antilla, Laasko and Lumme (1965), in which the surface is assumed to be covered by paraboloidal holes or craters (Figure 1). The shape of each crater is completely defined by the parameter $Q = h/R$, where h is the crater depth (measured from the mean surface level) and R is its radius. The quantity Q is clearly a measure of the large scale roughness of the surface.

Using cartesian coordinates as shown in Figure 1, with the XY plane coinciding with the mean surface, the direction of ε in the XZ plane, and the Z-axis along the axis of the paraboloid, the equation of the paraboloid is:

$$z = \frac{h}{R^2}(x^2 - y^2) - h. \tag{1}$$

We shall study the effects of surface roughness by calculating the photometric properties of a family of model surfaces each completely covered by craters of a given shape factor Q. It will be assumed that any real surface can then be approximated by considering an appropriate distribution of Q's. Such an approach is obviously deficient in that it does not allow well for crater overlap, but has the important advantage that it does deal with shadowing exactly within the framework of the model.

Thus although we do not claim that our approach is necessarily adequate to deal with the photometric properties of a real randomly rough surface, we do believe that it is useful in understanding what effects large scale surface roughness may have on the observed photometric properties of a surface. Note that our approach differs from the usual formulation used in radar astronomy where the rough surface is specified in terms of the distribution of height deviations (assumed small) from a mean level and shadowing is either neglected or treated approximately. Since we wish to treat shadowing exactly this approach is not useful in our context.

Now consider a particular point P within a crater of radius R, and shape factor Q. The conditions that this point is both illuminated and seen may be written down, following Hämeen-Antilla et al. (1965), as:

$$x^2 + y^2 \leq R^2 \tag{2}$$

$$(x - \frac{R^2}{h} \cot \varepsilon)^2 + y^2 \geq R^2 \tag{3}$$

$$(x - \frac{R^2}{h} \cot i \cos A)^2 + (y - \frac{R^2}{h} \cot i \sin A)^2 \geq R^2 \tag{4}$$

where A is the azimuth, and is related to the phase angle α, by:

$$\cos A = \frac{\cos \alpha - \cos i \cos \varepsilon}{\sin i \sin \varepsilon} \quad (0 \leq A \leq 180°). \tag{5}$$

Equation (2) assures that the point is within the crater, equation (3) that it is illuminated, and equation (4) that it is seen. Note that by the above definition of azimuth, in the case that i and ε are coplanar, A = 0° if they lie on the same side of the normal, and A = 180° if they do not.

At the point P the angles of incidence i* and of observation ε*, with respect to the local normal are given by:

$$\cos i^* = \frac{\cos i - 2 \sin i \{X \cos A + Y \sin A\}}{C} \tag{6}$$

and

$$\cos \varepsilon^* = \frac{\cos \varepsilon - 2X \sin \varepsilon}{C} \tag{7}$$

where,

$$X = \frac{h}{R^2}\, x$$

$$Y = \frac{h}{R^2}\, y$$

and $$C = \{1 + 4(X^2 + Y^2)\}^{1/2}$$

The element of surface area at P is given by:

$$d\sigma = C\, dxdy.$$

If the scattering at the point P is described by Minnaert's law, that is, if

$$B(i^*,\varepsilon^*)\cos\,\varepsilon^* = B_o(\cos\, i^*\, \cos\, \varepsilon^*)^k$$

then the apparent brightness averaged over the entire crater will be

$$(8) \qquad B(i,\varepsilon,\alpha) = \frac{\iint B(i^*,\varepsilon^*)\, \cos\, \varepsilon^*\, d\sigma}{\iint \cos\, \varepsilon\, d\sigma}$$

and normalizing so that $B_o = 1$, we have

$$(9) \qquad B(i,\varepsilon,\alpha)\, \cos\, \varepsilon = \frac{1}{\pi R^2} \iint (\cos\, i^*\, \cos\, \varepsilon^*)^k d\sigma$$

where the integration in (8) and (9) is carried out over the entire crater. We have assumed that the surface is dark enough that multiple reflections within craters can be neglected.

The effects of large-scale surface roughness on the photometric characteristics of a surface can now be studied

by selecting k, Q, α, and A. (It is intuitively clear that for a cratered surface the effects of shadows will be azimuth-dependent). We have written a computer program to evaluate equation (9) subject to conditions (2) - (4), using a 50 X 50 grid over the crater. Having specified k, Q, α, and A we select an (i,ε) pair consistent with the azimuth equation (5), and evaluate cos i* and cos ε* at all grid points which satisfy conditions (2) - (4). Using these points, (9) is evaluated to give $B(i,\varepsilon,\alpha)\cos\alpha$ for this (i,ε) pair. This procedure is repeated for a number of such pairs and the results are plotted on a log (B cos ε) vs log (cos i cos ε) graph to which a straight line is fitted by least squares. The slope of this line $k^* = k^*(A,\alpha,Q,k)$ is the effective Minnaert exponent for this rough surface. An example of such a calculation is shown in Figure 2, for k = 0.5, Q = 1.0, $\alpha = 22°$ and A = 10°. The resulting k* = 0.70 is well-defined and differs significantly from k.

Since such calculations are time-consuming we have decided to treat only three specific cases in detail. First, the case k = 0.5 and $\alpha = 22°$; second, k = 0.7 and $\alpha = 22°$; and last k = 1.0 and $\alpha = 90°$. The first two cases are relevant to the paper by Young and Collins (1971) refered to above, and the last to the UV photometry of Martian bright areas by Hord (1971).

It should be noted that in all the subsequent figures the dashed curves are smooth fits to the black dots which represent the calculated points. We believe that in all cases the density of calculated points is large enough to assure that the dashed curves do not deviate significantly from the true

behavior of k*.

Finally, it should be stressed that even though we have normalized B_o to unity, B_o^*, the intercept of the Minnaert plot corresponding to k*, will in general differ from unity. This is certainly important in calculating effective average values of k* (as in Figures 5 and 8), but the variation of B_o^* is not remarkable and we have decided not to present it in detail. Suffice it to say that for instance for Q = 0.2, B_o^* ranges from 1.04 to 1.00 for k = 0.5, and from 1.00 to 0.98 for k = 0.7, as A ranges from 0° to 180°. For Q = 0.4 the corresponding variations are from 1.04 to 0.99 for k = 0.5, and 0.94 to 0.92 for k = 0.7.

3. Case 1: Phase angle 22°, k = 0.5

The effects of increasing surface roughness on k* are shown in Figures 3a and 3b. It is clear that there is a strong dependence on azimuth. Note that there is an essential singularity at A = 90° inherent in the Minnaert scattering law, since from (5), A = 90° implies cos i cos ε = cos α = constant at a given phase angle. Hence all points on a Minnaert plot fall on a vertical line and the slope is indeterminate.

In Figure 4 we have plotted k* as a function of azimuth for Q = 0.2, 0.5, 0.8, and 1.0. The singularity at A = 90° is such that $k^* \to -\infty$ as $A \to 90°$ from below, and $k^* \to +\infty$ as $A \to 90°$ from above. It is clear that the tendency is for k* to increase from its Q = 0 value, except as $A \to 90°$ from below.

Figure 5 shows $\langle k^* \rangle_A$, (k* averaged over azimuth), as a function of the roughness parameter Q. The weighing factors used in the averaging are determined by the distribution of azimuths over a disk at a phase angle of 22°, neglecting the interval A = 80° - 100°, where the changes in k* are severe but seem to cancel themselves, at least for $Q \leq 0.5$.

The trend is for $\langle k^* \rangle_A$ to increase with Q from $\langle k^* \rangle_A = 0.50$ at Q = 0 to $\langle k^* \rangle_A = 0.66$ at Q = 1.0.

Q is related to the maximum slope on the surface, $\tan \theta_{max}$, by the relation

$$\tan \theta_{max} = 2Q.$$

If the maximum slope is constrained to be less than 35° (a typical angle of repose for loose materials), $Q \leq 0.35$. Thus, for example, if we choose a gaussian distribution of Q's, peaked at $Q = 0.2$, with $\sigma = 0.1$, we find

$$\langle k^* \rangle_{A,Q} = 0.55$$

for $k = 0.5$ and $\alpha = 22°$.

Judging from Mariner 6 and 7 close encounter photographs such as 6N8, there may be regions on Mars which are considerably rougher than a surface with $\langle Q \rangle = 0.2$ and $\sigma = 0.1$. In such a case the departure of k* from k will be even more pronounced.

4. Case 2: Phase angle 22°, k = 0.7

The effects of increasing surface roughness on k* are shown in Figures 6a and 6b. Again there is a strong azimuthal dependence, but unlike the $k = 0.5$ case, here the general trend is for k* to be lower than k. In Figure 7 we have shown k* as a function of azimuth for $Q = 0.2$, 0.5, 0.8 and 1.0. Figure 8 shows k* averaged over azimuth (as in Section 3) as a function of Q. The overall trend is for $\langle k^* \rangle_A$ to decrease with increasing Q, from $\langle k^* \rangle_A = 0.70$ at $Q = 0$ to $\langle k^* \rangle_A = 0.56$ at $Q = 1.0$.

If we again assume that the distribution of Q's over the surface is gaussian, centered at $Q = 0.2$ and has $\sigma = 0.1$,

$$\langle k^* \rangle_{A,Q} = 0.69.$$

5. Case 3: Phase angle 90°, k = 1.0

In this case the azimuth A must be greater than 90°. Figure 9 shows k* as a function of Q, for azimuths ranging from 100° to 180°. For small Q, say $Q \leq 0.3$, $k^* \simeq k$ independent of Q or A. However, for $Q > 0.5$ the difference between k* and k becomes large at all azimuths larger than 110°. For instance, at azimuths between 135° and 180°, $k^* \simeq 0.7$ for a surface with $Q = 0.8$.

6. Conclusions

It is clear from the above examples that the effects of macroscopic surface roughness must be considered in any detailed study of the spatial and temporal variations in k* on the surface of Mars or other planets. In situations where measurements are made over a limited range of azimuths, k* may differ considerably from k even for small surface roughness. For example, Figure 3a shows that, at $\alpha = 22°$ and $A < 20°$, $k^* - k \simeq 0.1$ even for Q as small as 0.2.

There are probably locales on Mars (parts of the chaotic terrain, for example) where the surface is macroscopically very rough. If for instance $Q \sim 0.5$, then starting with a $k = 0.50$ one may easily observe a $k^* = 0.60$, while starting with $k = 0.70$ one may find a $k^* = 0.65$.

The general trend of the $k = 0.7$ curves (at $\alpha = 22°$) is for k* to decrease to and below 0.5 as the surface becomes progressively rougher. Thus the possibility arises that the

difference between the k*'s of Ophir (0.63-0.71) and Elysium (0.55-0.56) may be largely due to the greater surface roughness of Elysium.

The general trend of the k = 0.5 curves (at $\alpha = 22°$) is for k* to increase above 0.5 as the surface becomes rougher. It is likely that for Mars at $\alpha = 22°$, k lies closer to 0.7 than to 0.5 (Young and Collins, 1971), so that the former case is probably more relevant. It is interesting that, for that case, values of k* ranging from 0.7 to below 0.5 may be obtained by varying the surface roughness Q and the azimuth A.

Azimuthal dependence of the scattered light, and therefore of k*, provides a sensitive test for the influence of macroscopic roughness effects on the photometric properties. If no azimuthal dependence is found, it is safe to assume that such effects are not important, and that k* is very close to k. In this case, observed values of k* may be used directly to infer the small-scale texture of the surface.

On the other hand, if k* is found to be azimuth-dependent, the effects of macroscopic surface roughness are important, and observed regional variations in k* may only reflect differences in large scale roughness, and not in the microscopic properties of the surface.

The effects of moderate degrees of surface roughness on the <u>disk-integrated</u> photometric properties seem to be small. For example, for Case 1 ($\alpha = 22°$, k = 0.5), a typical disk-integrated k* ($\equiv \langle k^* \rangle_{A,Q}$) for a likely distribution of Q's is

0.55 (Section 3); a similar calculation for Case 2 ($\alpha = 22°$, $k = 0.7$) gives $\langle k^* \rangle_{A,Q} = 0.69$ (Section 4).

Acknowledgement:

We are indebted to Carl Sagan and Laird Whitehill for helpful comments and suggestions. This research was supported in part by NASA JPL Contract 952487 and in part by NASA Grant NGR 33-010-098. One of us, L. Wasserman, was supported by a National Science Foundation Traineeship during the course of this investigation.

References

Hämeen-Antilla, K. A., Laakso, P. and Lumme, K. (1965) "The shadow effect in the phase curves of lunar type surfaces." Ann. Acad. Scien. Fennicae Ser. A., No. 172.

Hord, C. W. (1971) "Mariner 6 and 7 ultraviolet photometry of the polar caps and the bright regions of Mars." Presented at the 14th COSPAR Meeting. Seattle.

Young, A. T. and Collins, S. A. (1971) "Photometric properties of the Mariner cameras and of selected regions of Mars." JGR 76, 432.

FIGURE CAPTIONS

Figure 1: Scattering geometry and schematic diagram of a single crater of the model surface.

Figure 2: Minnaert plot for the case $k = 0.5$, $\alpha = 22°$, $A = 10°$. ($B_o \equiv 1$). Solid line: $Q = 0$; dashed line: least squares fit to points generated by the computer program for the case $Q = 1.0$. ($k^* = 0.7$ and $B_o^* = 0.98$).

Figure 3a: The variation of k^* with the surface roughness parameter Q for azimuths of 0°, 10°, 20°, 30°, 45°, 60°, and 80°. This is for Case 1 ($\alpha = 22°$, $k = 0.5$). In this, and in all subsequent figures, the dashed curves are smooth fits to the calculated points which are shown as black dots.

Figure 3b: Same as Figure 3a, but for azimuths of 100°, 120°, 135°, 150° and 180°.

Figure 4: The variation of k^* with azimuth for $Q = 0.2$, 0.5, 0.8 and 1.0. Note the singularity at $A = 90°$ discussed in the text. This is for Case 1 ($\alpha = 22°$, $k = 0.5$).

Figure 5: The value of k^* averaged over azimuth for a disk at $\alpha = 22°$ (see text), as a function of the roughness parameter Q. (Case 1: $\alpha = 22°$, $k = 0.5$).

Figure 6a: The variation of k^* with the surface roughness parameter Q, for azimuths of 0°, 10°, 20°, 30°, 40°, 60° and 80° (Case 2: $\alpha = 22°$, $k = 0.7$).

Figure 6b: Same as Figure 6a, but for azimuths of 100°, 120°, 135°, 150° and 180°.

Figure 7: The variation of k* with azimuth for Q = 0.2, 0.5, 0.8, 1.0 (Case 2: $\alpha = 22°$, k = 0.70).

Figure 8: The value of k* averaged over azimuth for a disk at $\alpha = 22°$ (see text), as a function of the roughness parameter Q. (Case 2: $\alpha = 22°$, k = 0.70).

Figure 9: The variation of k* with the surface roughness parameter Q, for azimuths of 100°, 110°, 135°, 150° and 180°. (Case 3: $\alpha = 90°$, k = 1.0). Note that in this case the azimuth must exceed 90°.

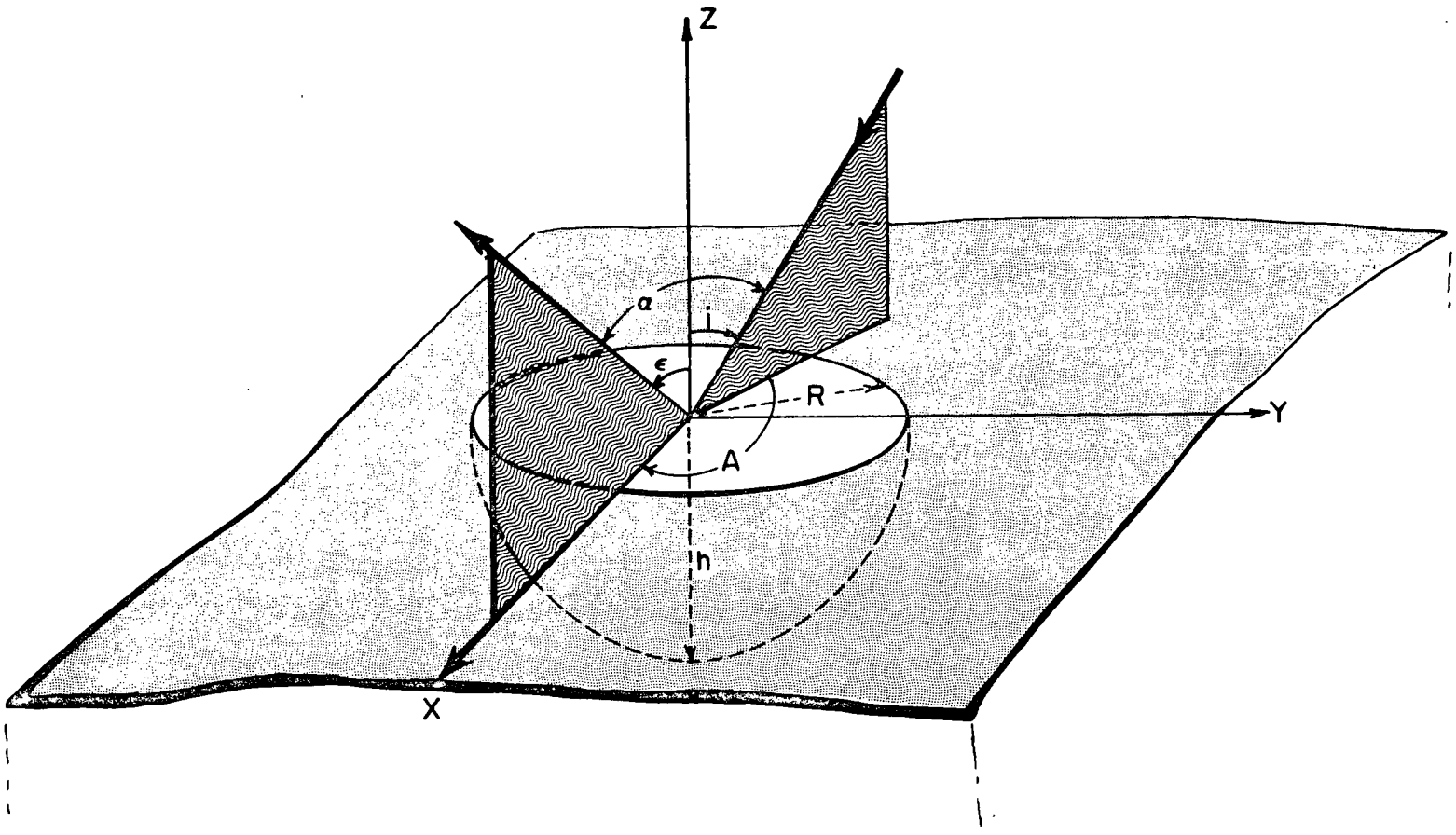

Figure I.

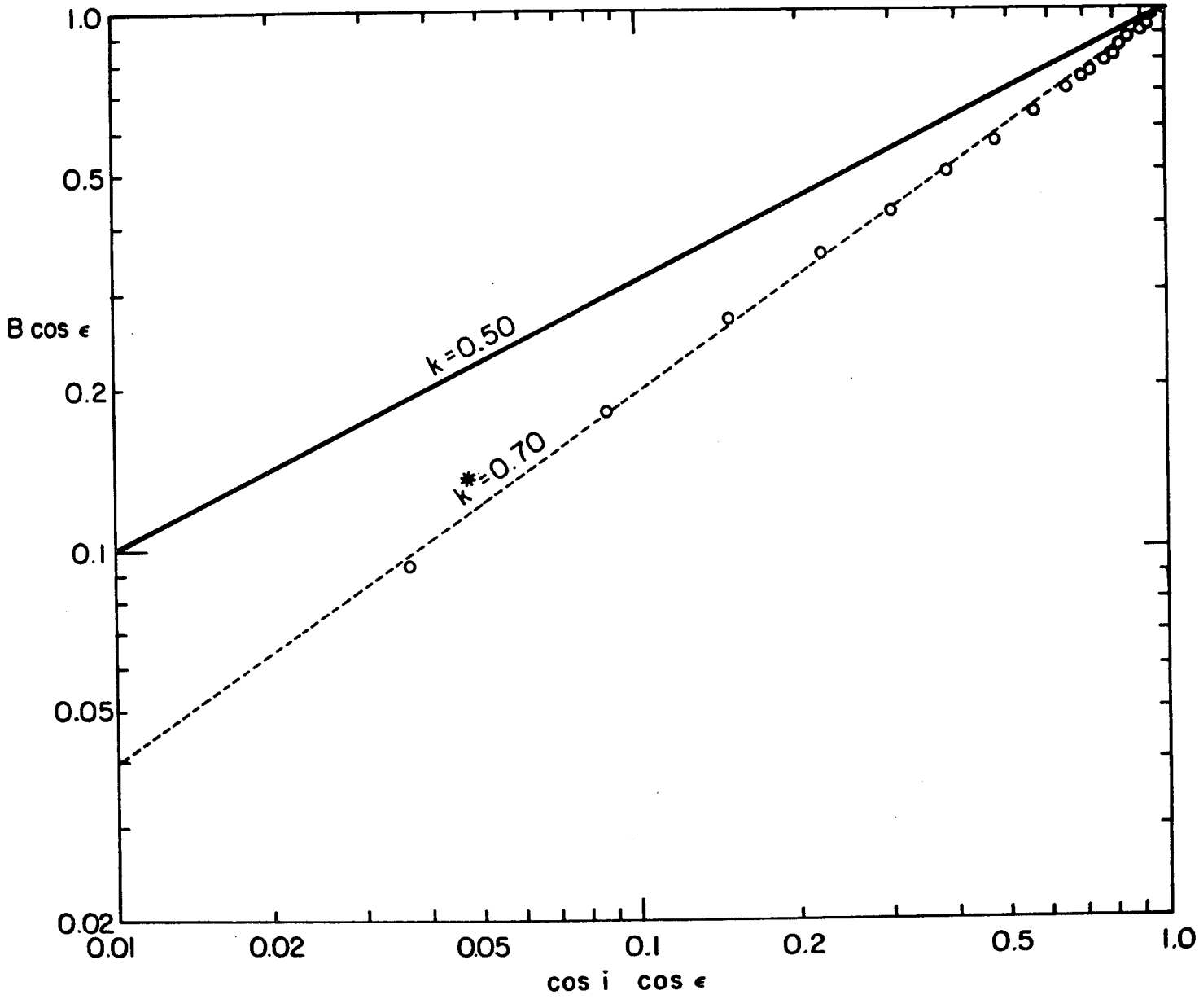
1.0
0.5
B cos ϵ
0.2
0.1
0.05
0.02
k=0.50
k*=0.70
0.01
0.02
0.05
0.1
0.2
0.5
1.0
cos i cos ϵ

Figure 2.

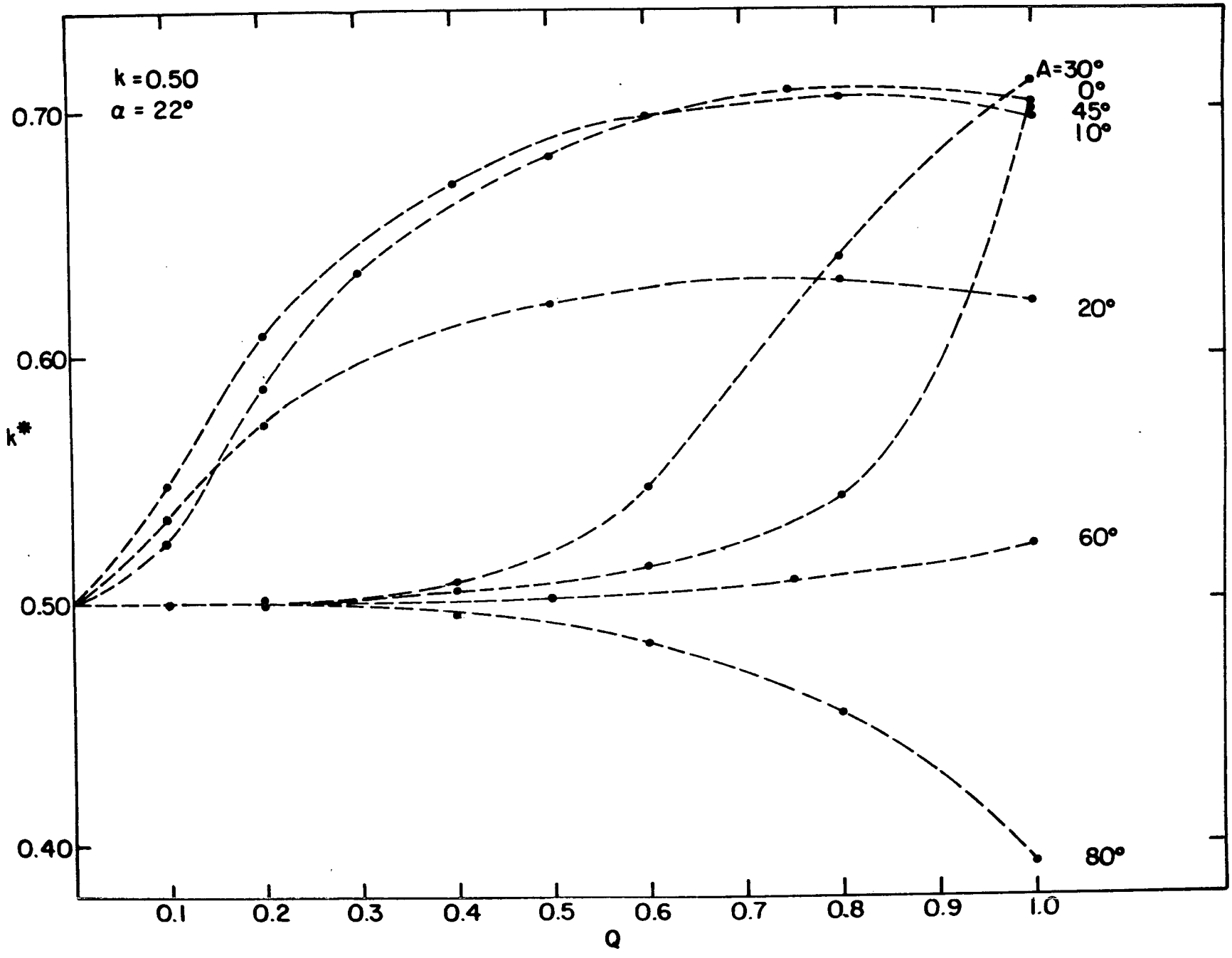
k = 0.50
α = 22°
A=30°
0°
45°
10°
20°
60°
80°
0.70
0.60
0.50
0.40
k*
0.1
0.2
0.3
0.4
0.5
0.6
0.7
0.8
0.9
1.0
Q

Figure 3a.

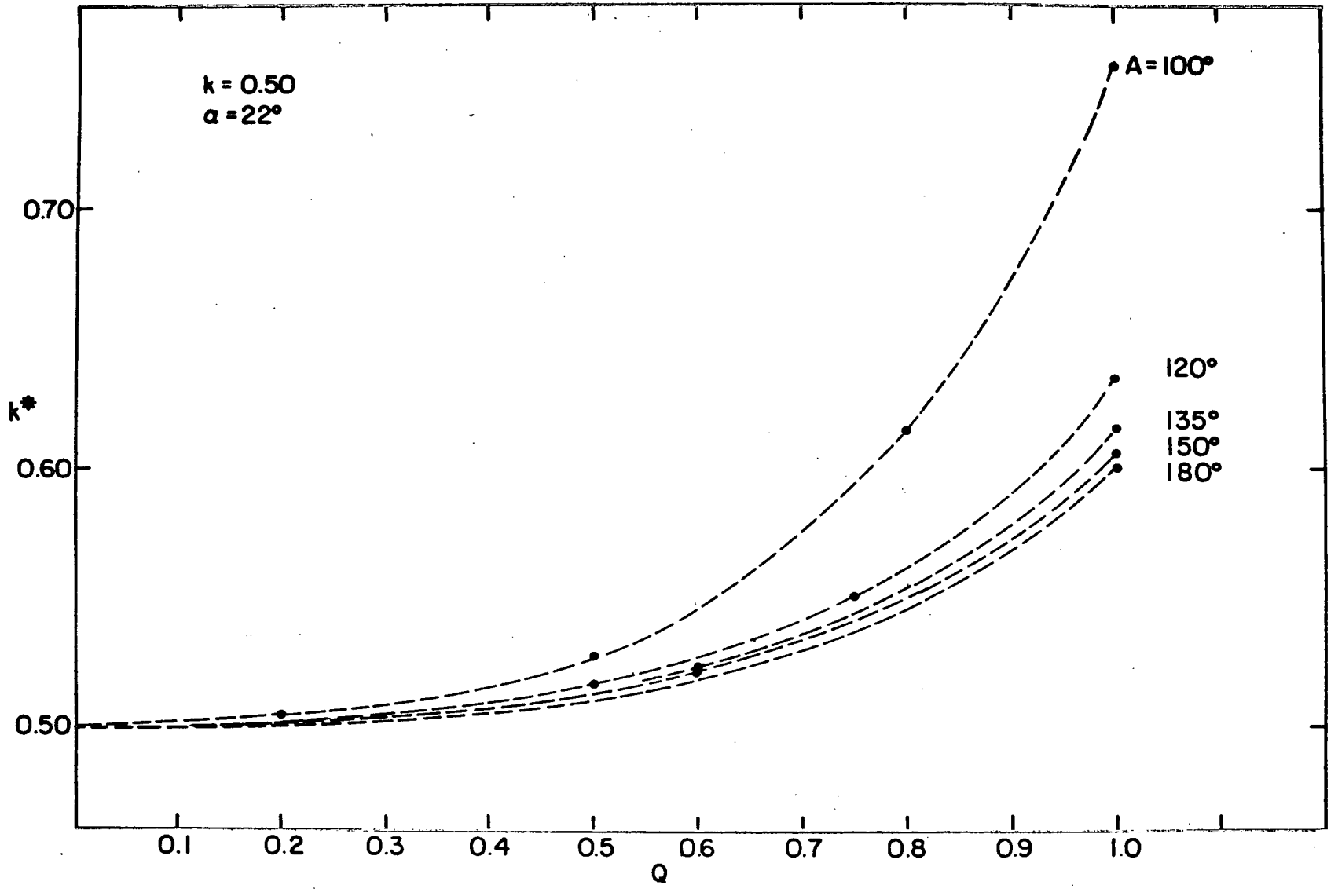
k = 0.50
α = 22°
A = 100°
120°
135°
150°
180°
k*
0.70
0.60
0.50
0.1
0.2
0.3
0.4
0.5
0.6
0.7
0.8
0.9
1.0
Q

Figure 3b.

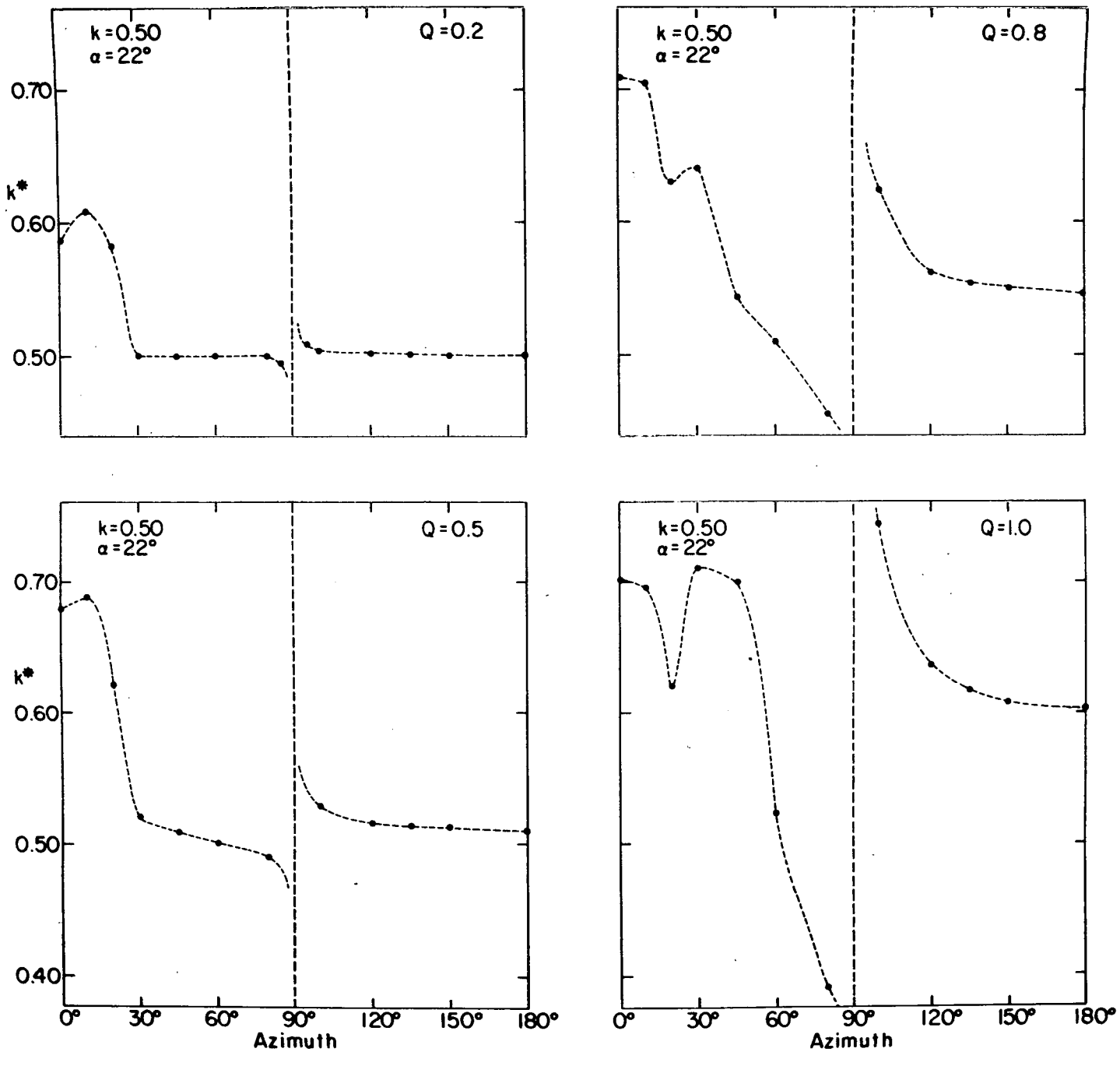
k=0.50
α=22°
Q=0.2
k=0.50
α=22°
Q=0.8
k=0.50
α=22°
Q=0.5
k=0.50
α=22°
Q=1.0
k*
0.70
0.60
0.50
0.40
0°
30°
60°
90°
120°
150°
180°
Azimuth

Figure 4.

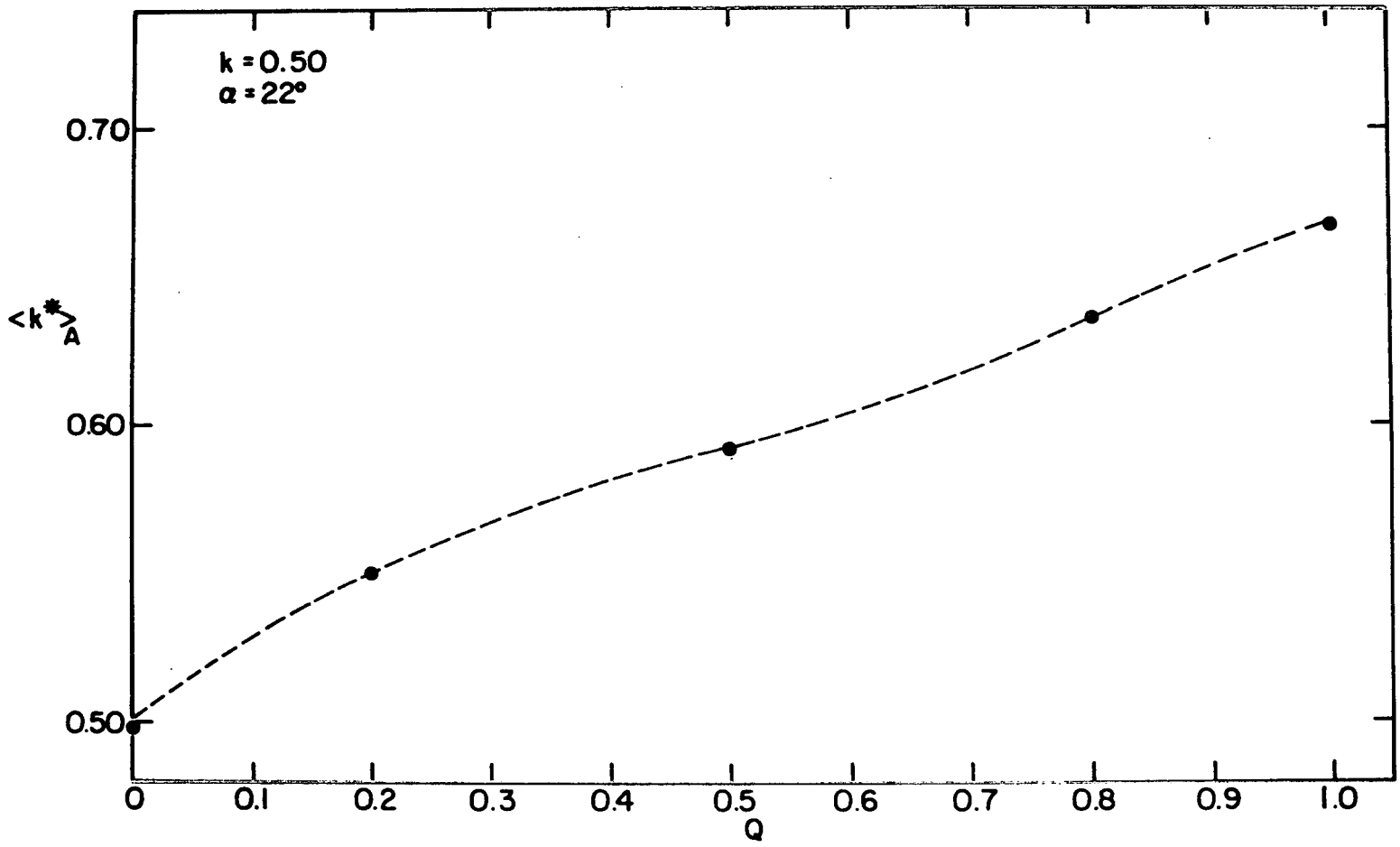
k = 0.50
α = 22°
0.70
0.60
0.50
$\langle k^* \rangle_A$
0
0.1
0.2
0.3
0.4
0.5
0.6
0.7
0.8
0.9
1.0
Q

Figure 5.

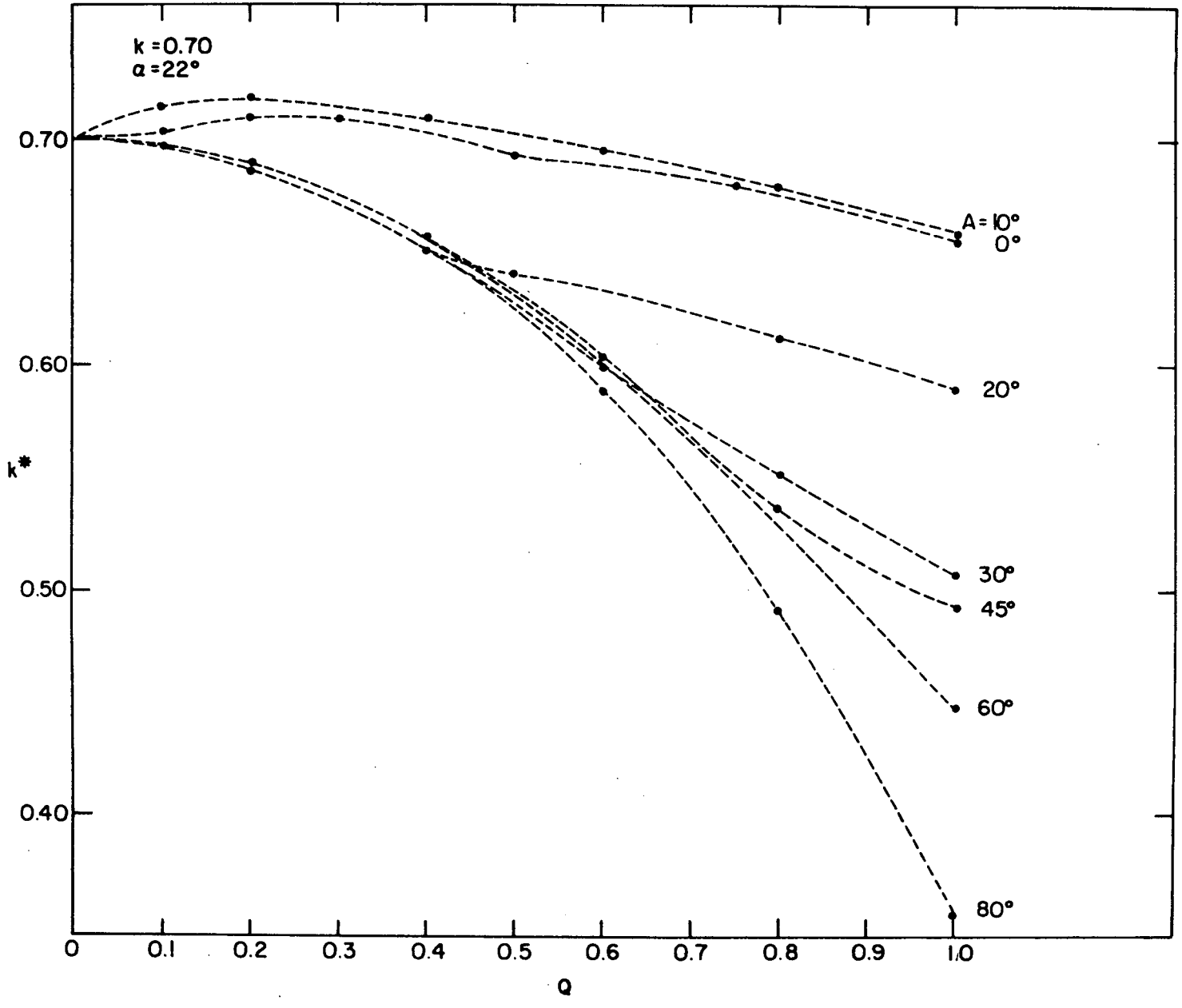
k =0.70
α =22°
0.70
0.60
0.50
0.40
k*
0
0.1
0.2
0.3
0.4
0.5
0.6
0.7
0.8
0.9
1.0
Q
A = 10°
0°
20°
30°
45°
60°
80°

Figure 6a.

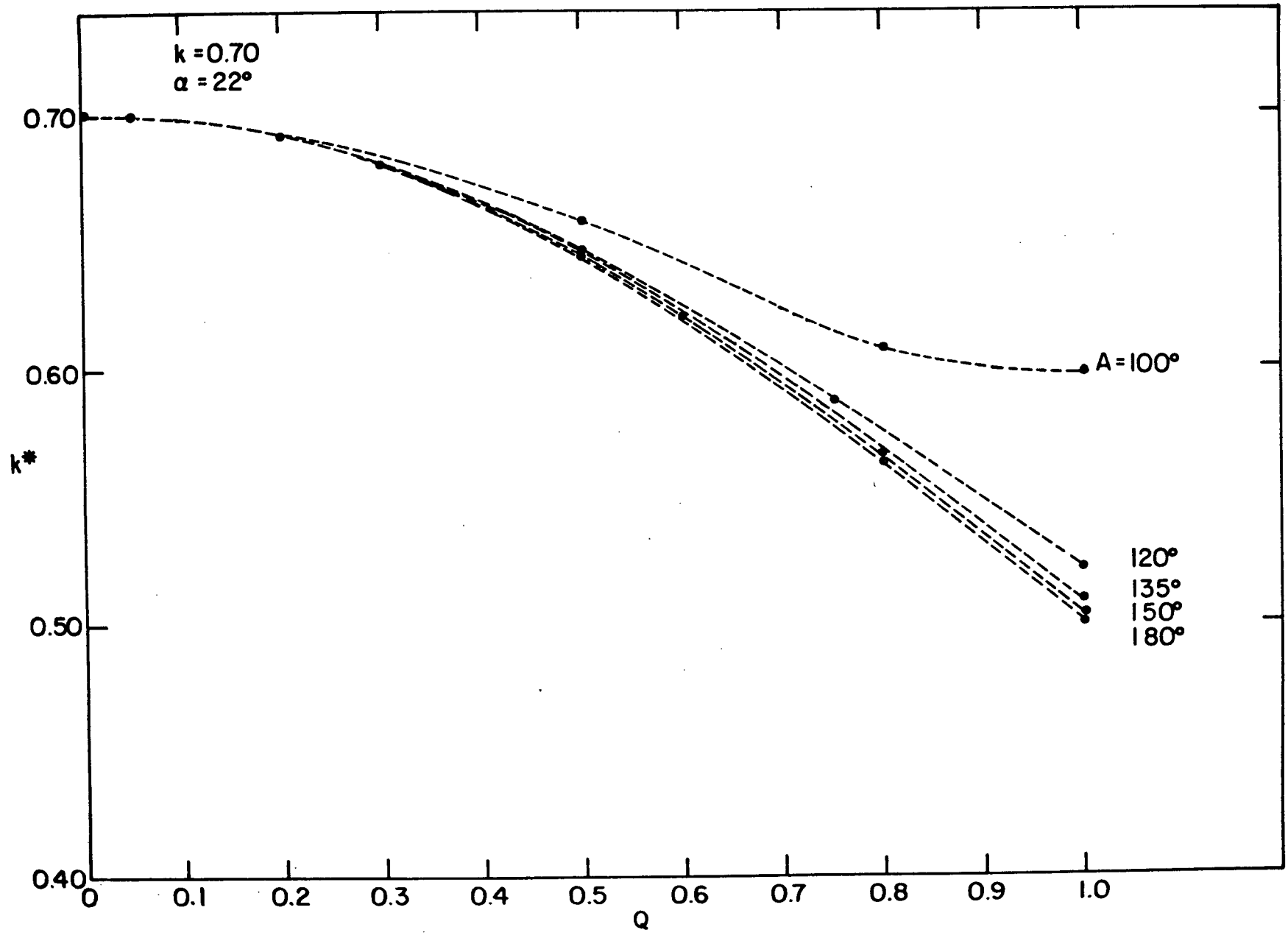
k =0.70
α = 22°
0.70
0.60
0.50
0.40
k*
0
0.1
0.2
0.3
0.4
0.5
0.6
0.7
0.8
0.9
1.0
Q
A=100°
120°
135°
150°
180°

Figure 6b.

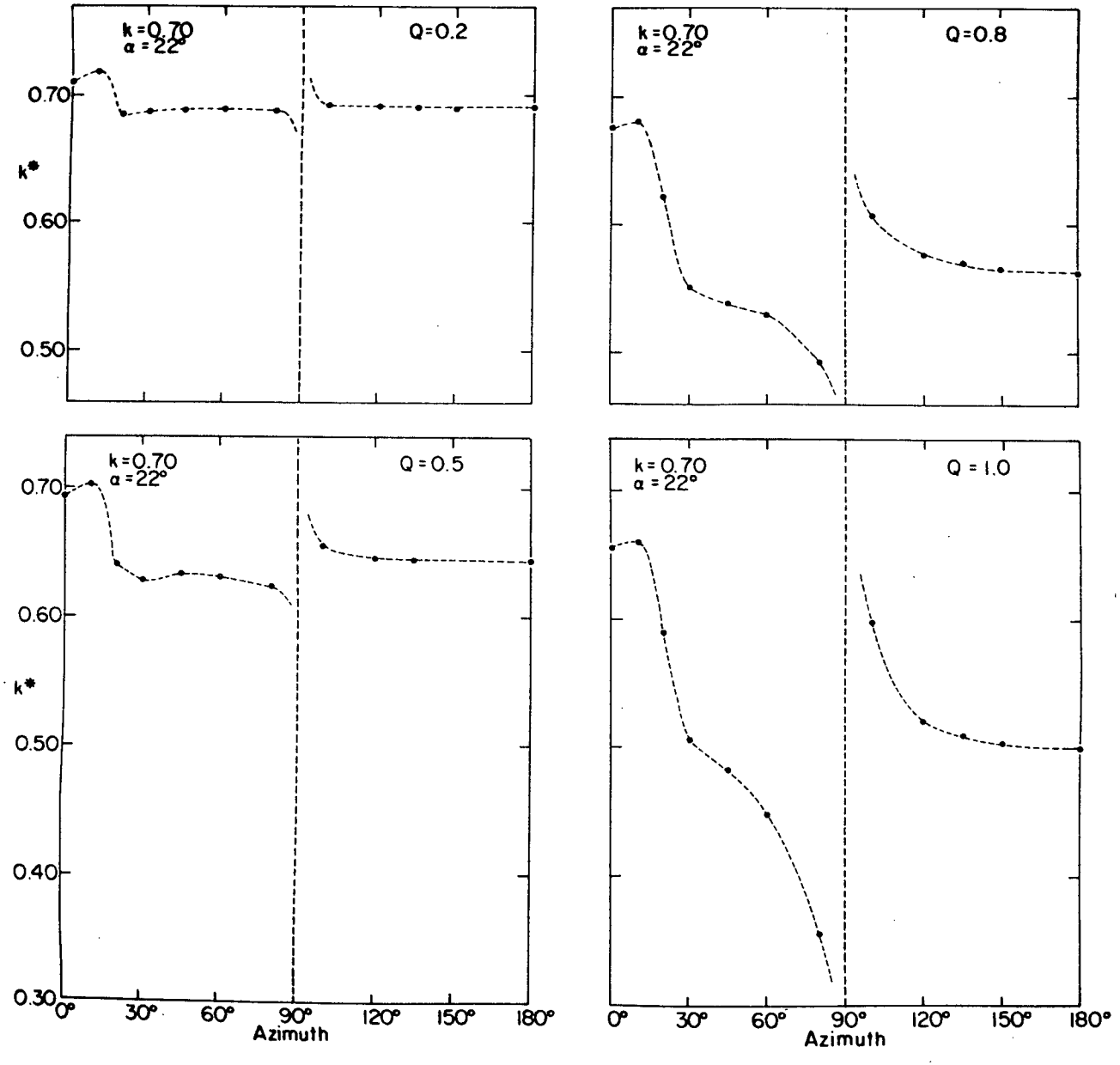
k=0.70
α=22°
Q=0.2
k=0.70
α=22°
Q=0.8
k=0.70
α=22°
Q=0.5
k=0.70
α=22°
Q=1.0
k*
0.70
0.60
0.50
0.40
0.30
0°
30°
60°
90°
120°
150°
180°
Azimuth

Figure 7.

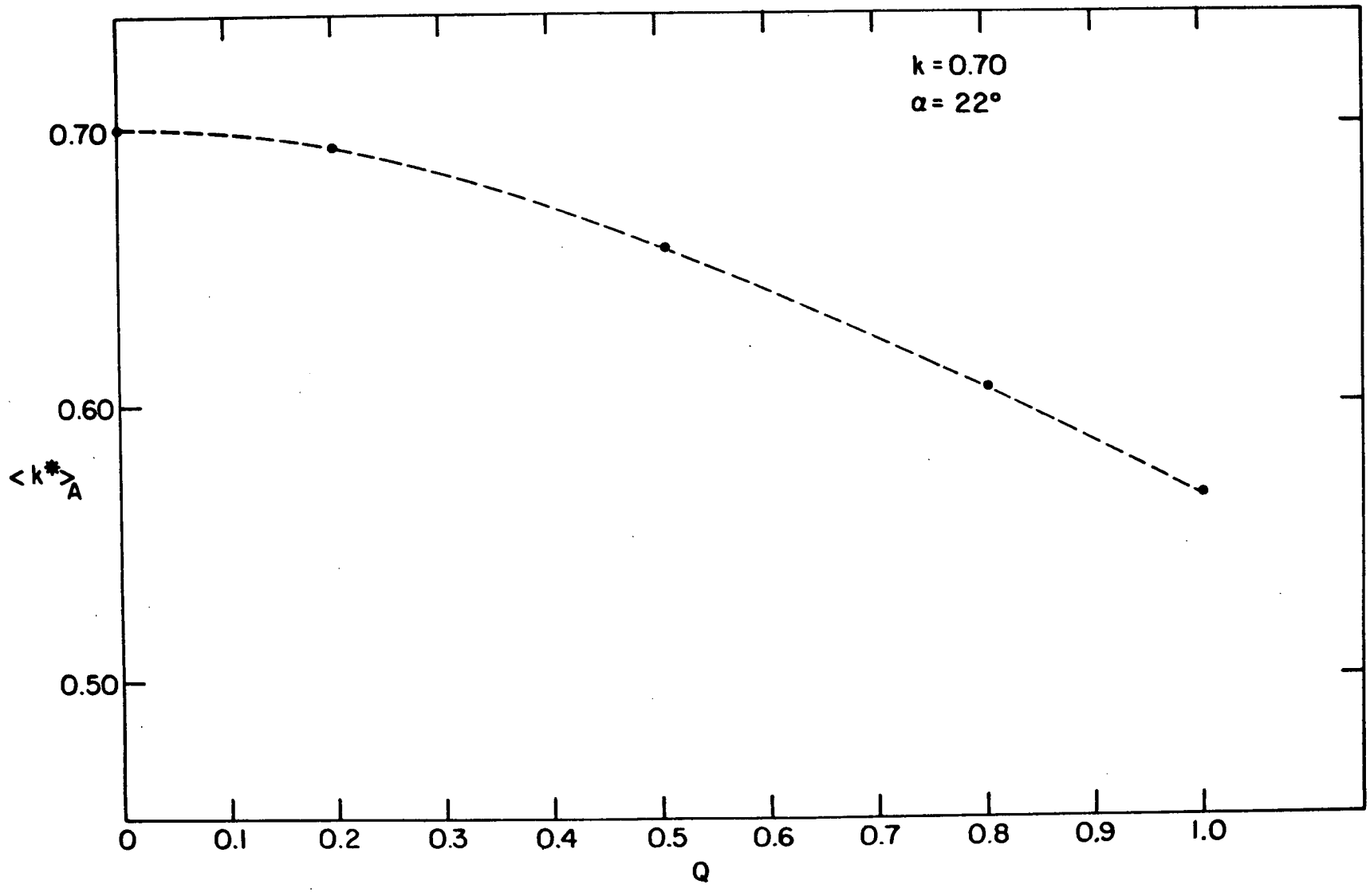

Figure 8.

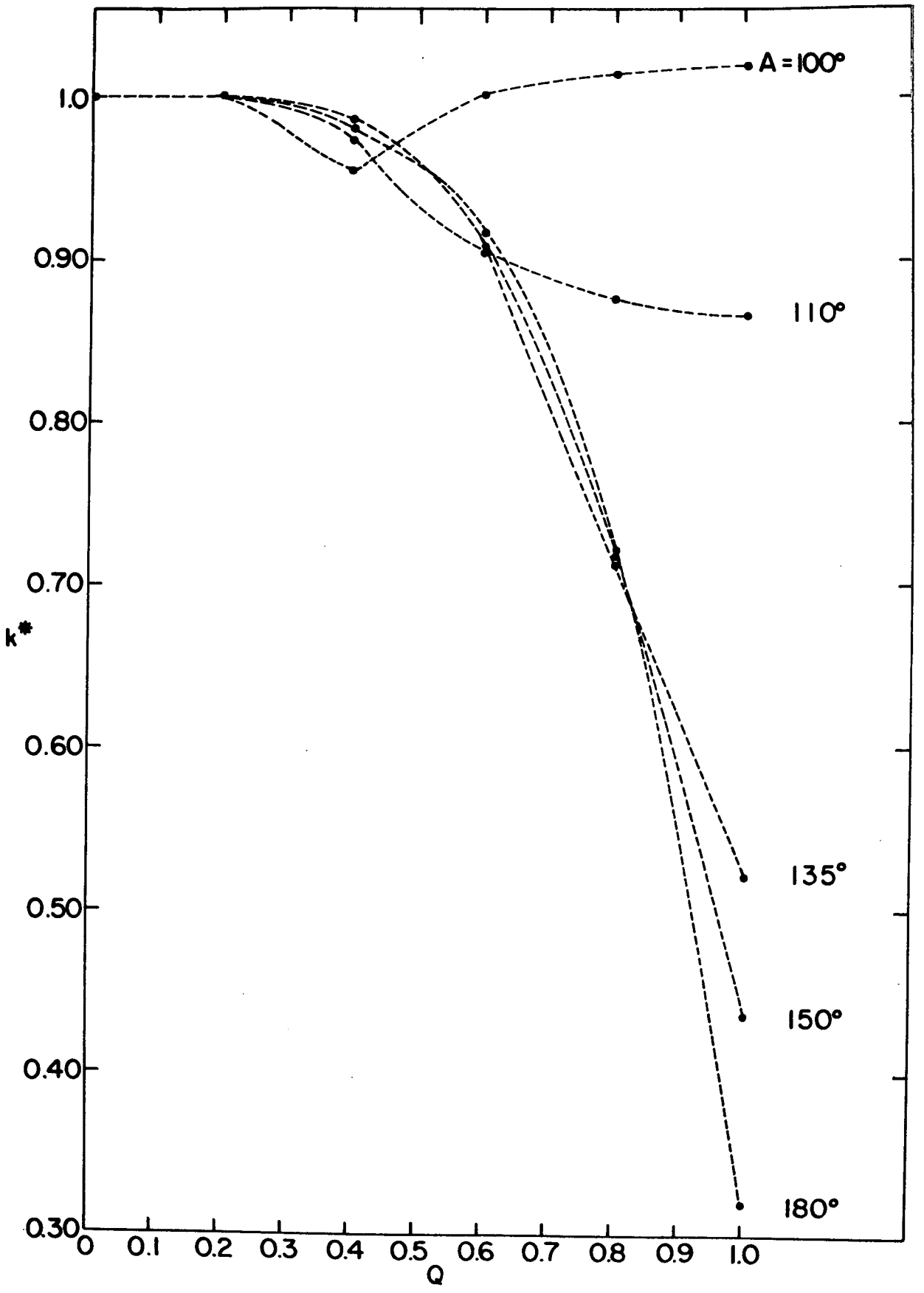
A = 100°
110°
135°
150°
180°
1.0
0.90
0.80
0.70
0.60
0.50
0.40
0.30
k*
0
0.1
0.2
0.3
0.4
0.5
0.6
0.7
0.8
0.9
1.0
Q

Figure 9.